Freundlich, Dekel, Jiang et al., in prep.
Jiang, Dekel, Freundlich et al., in prep.

Core formation in dark matter haloes and Ultra Diffuse Galaxies

Jonathan Freundlich[1], Fangzhou Jiang[1], Avishai Dekel[1,2], Sharon Lapiner[1], Tomer Nussbaum[1], Aaron Dutton[3] & Andrea Macciò[3,4]

[1]Centre for Astrophysics and Planetary Science, Racah Institute of Physics, The Hebrew University, Jerusalem 91904, Israel
[2]Santa Cruz Institute for Particle Physics, University of California, Santa Cruz, CA 95064, USA
[3]New York University Abu Dhabi, PO Box 129188, Saadiyat Island, Abu Dhabi, United Arab Emirates
[4]Max Planck Institute für Astronomie, Königstuhl 17, 69117 Heidelberg, Germany

האוניברסיטה העברית בירושלים
THE HEBREW UNIVERSITY OF JERUSALEM

ABSTRACT

While cold dark matter numerical simulations predict 'cuspy' density profiles for dark matter halos, observations favor shallower 'cores'. The introduction of baryonic physics alleviates this discrepancy as feedback-driven episodes of impulsive gas outflow and inflow affect the dark matter distribution. Such episodes also affect the stellar distribution and can explain the formation of Ultra Diffuse Galaxies (UDGs), which are ubiquitous in dense environments and also detected in the field, characterized by stellar masses typical of dwarf galaxies while being as extended as the Milky Way. We present a simple theoretical model for the response of dark matter haloes and UDGs to episodes of gas inflows and outflows, which provides a theoretical framework to understand the transition from dark matter cusps to cores and the formation of UDGs in the field. We further analyze UDGs in cosmological zoom-in simulations both in the field and in galaxies groups. For galaxies in the field, we find that the host haloes of UDGs have typical spin but lower concentration than non-UDGs, and that UDGs are generally more dark-matter dominated inside their effective radius. For UDGs in galaxy groups, we find that the only significant radial gradient is in specific star formation rate, UDGs being more quiescent towards the center. On appropriate orbits, satellite dwarfs can become UDGs after pericenter passage, where they lose most of the cold gas, quench, and get puffed up by tidal shocks. The weak radial trend of stellar mass and size are the outcome of the combined effect of tidal stripping, puffing up, and disruption of low-mass, diffuse systems.

The cusp-core discrepancy

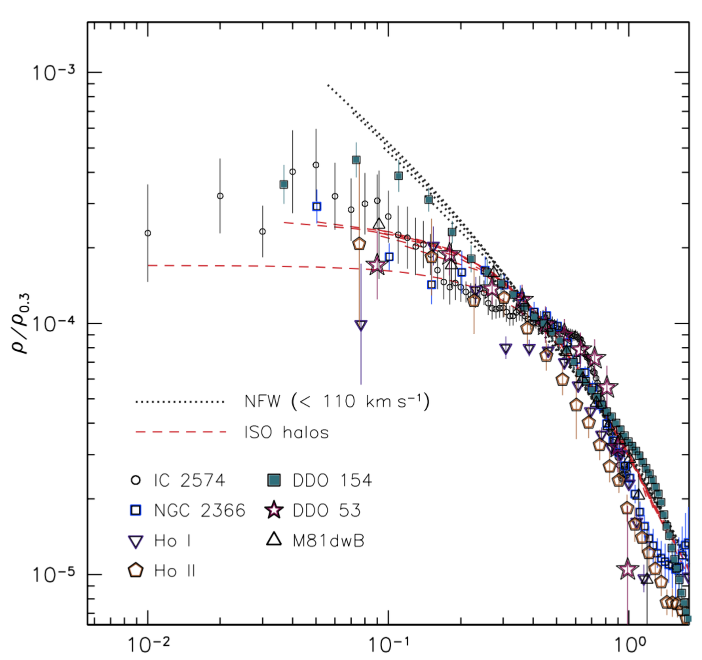

Figure 1. Observations of dwarf galaxies favor dark matter cores instead of the steeper NFW cusps predicted by cold dark matter simulations (Oh et al. 2011).

Including baryonic processes such as feedback from stars and active galactic nuclei in hydrodynamical simulations enables to reproduce cores and thus alleviates the discrepancy (e.g., Governato et al. 2010, Teyssier et al. 2013).

Ultra Diffuse Galaxies

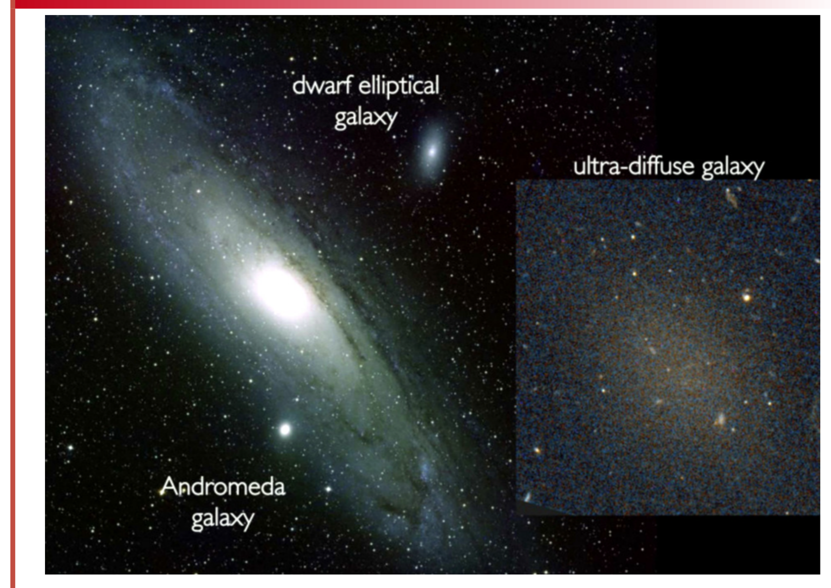

Figure 2. Deep imaging of nearby clusters reveal the existence of a population of low central surface brightness Ultra Diffuse Galaxies (UDGs) with stellar masses of dwarf galaxies ($7 < \log(\mathrm{M_{star}}/\mathrm{M_\odot}) < 9$) and effective radii comparable to that of the Milky Way (Van Dokkum et al. 2015): $7 < \log(\mathrm{M_{star}}/\mathrm{M_\odot}) < 9$; $1 < \mathrm{r_{eff}}/\mathrm{kpc} < 5$.

Possible formation scenarii include UDGs being failed Milky Way-like galaxies that lost their gas after forming their first stars (van Dokkum et al. 2015), the high-spin tail of the dwarf galaxy population (Amorisco & Loeb 2016), tidal debris from mergers or tidally disrupted dwarfs (Greco et al. 2018) or galaxies whose spatial extend is due to episodes of inflows and outflows from stellar feedback (Di Cintio et al. 2017).

A toy model based on episodes of inflows and outflows

Repeated mass fluctuations induced by stellar winds, supernova explosions and active galactic nucleai can dynamically 'heat' the dark matter (DM) distribution and lead to the formation of a core (Pontzen & Governato 2012). Similarly, episodes of inflows and outflows from stellar feedback can account for the formation of UDGs in the field by spatially extending both the stellar and the dark mater components (Di Cintio et al. 2017).

We present a simple theoretical model based on cycles of inflows and outflows that can both explain the formation of cores and of UDGs (Freundlich, Dekel, Jiang et al., in prep.), initially outlined by Dutton et al. (2016).

We consider the evolution of a spherical shell encompassing a collisionless mass M when a baryonic mass m is removed (or added) instantaneously at the center. The shell is initially at radius r_i and we express its potential, kinetic and total energy as it reacts to the mass variation according to the following steps:

1/Initial conditions at equilibrium:

$$E_i(r_i) = U_i(r_i) + K_i(r_i),$$

where the kinetic energy $K_i = 1.5\sigma_r^2$ is derived from the mass distribution through the Jeans equation

$$\frac{d(\rho\sigma_r^2)}{dr} = -\rho\frac{d\Phi}{dr},$$

assuming complete spherical symmetry and an anisotropy parameter $\beta = 0$.

2/Immediately after the change of mass, we assume that the potential adapts instantaneously to the mass variation while the velocities are frozen to their initial values:

$$E_t(r_i) = U_i(r_i) - Gm/r_i + K_i(r_i)$$

3/The system relaxes to a new state of equilibrium, the shell being now at r_f and its kinetic energy K_f expressed from the new mass distribution through the Jeans equation:

$$E_f(r_f) = U_f(r_f) - Gm/r_f + K_f(r_f)$$

Assuming $K = GM_{tot}/2r$ as in the virial equation and neglecting the contribution of the outer shells to the potential ($U = -GM/r$), Dutton et al. (2016) obtain

$$\frac{r_f}{r_i} = \frac{1+f}{1+2f} \text{ where } f = m/M.$$

More generally, given parametric functional forms for the collisionless contribution to the potential $U(r;p)$ and kinetic energy $K(r;p,m)$, we can obtain the final parameters p_f and the radii r_f of the different shells from given p_i, r_i by minimizing the difference between $E_t(r_i)$ and $E_f(r_f)$ – assuming energy conservation for shells encompassing a given collisionless mass between steps 2 and 3. We use the Dekel et al. (2017) parametrization of the mean density profile,

$$\overline{\rho}(r) = \frac{\overline{\rho_c}}{x^a(1+x^{1/2})^{2(3-a)}} \text{ with } x = r/r_s,$$

which matches density profiles as well as NFW, enables any inner slope a and provides an analytic expression for the potential.

A succession of adiabatic inflows and instantaneous such outflows leads to a flattening of the dark matter and stellar density profiles.

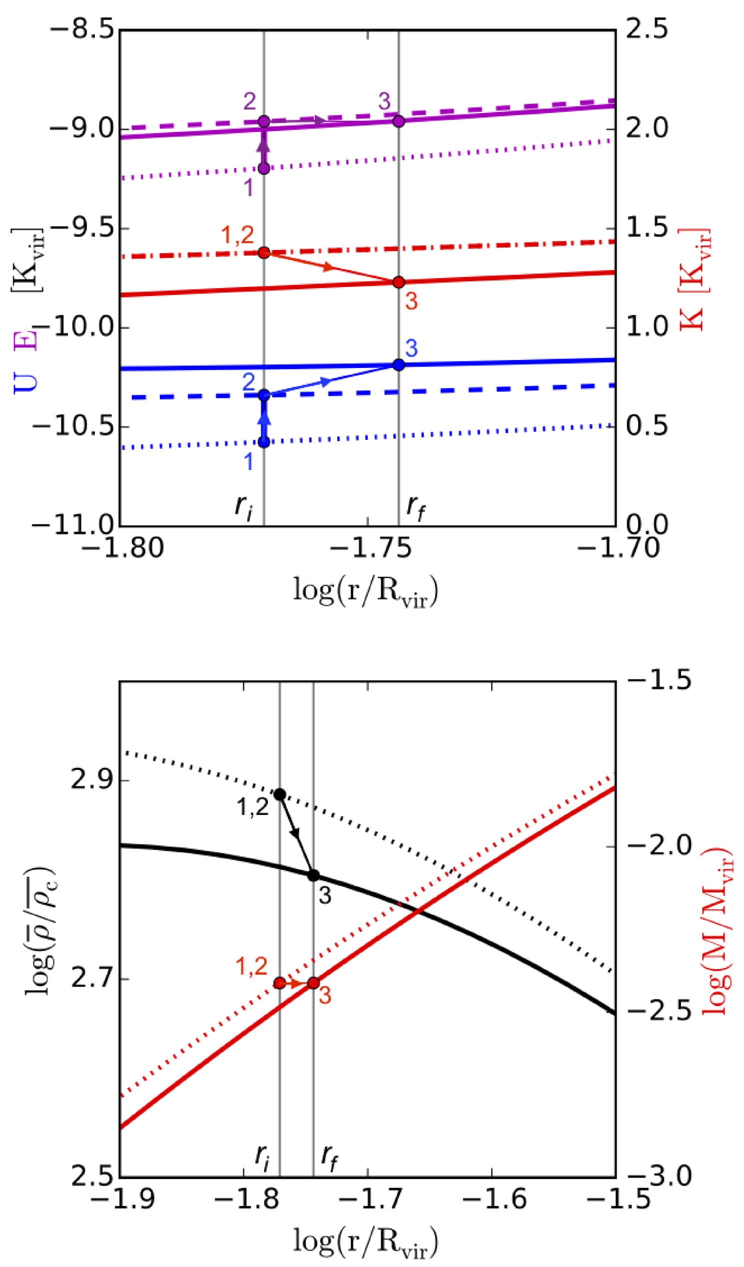

Figure 3. *Top*: Potential, kinetic and total energy at the different steps when mass is removed at the center (1: dotted; 2: dashed; 3: plain). *Bottom*: Corresponding evolution of the density and mass profiles, leading to the formation of a core.

The formation of field UDGs from feedback

We analyze field UDGs in the cosmological zoom-in NIHAO simulations (Wang et al. 2015), with an emphasis on their shape, host halo structure, and formation (Jiang, Dekel, Freundlich et al., in prep.):

The NIHAO simulations

- A set of ~90 field galaxies
- SPH improved Gasoline
- Halo masses $10^{9.5} - 10^{12.3}$
- Resolution 1% $\mathrm{R_{vir}}$
- Gas cooling, UV background heating, ionization, star formation, chemical enrichment
- Stellar feedback

- While their MW analogs are generally well described by an NFW profile, UDGs (defined with an effective radius $r_{eff} > 1.5$ kpc and a central V-band surface brightness > 24 mag.arcsec^{-2}) exhibit a significant dark matter core (Fig. 4).
- The host halo mass of UDGs is confined in the range $M_\mathrm{v} \sim 10^{10-11}M_\odot$ (Fig. 5) while their stellar mass is confined to a corresponding narrow range, in line with observations. This could result from the potential being too deep at higher masses, leading to contraction, while there are not enough outflows from feedback at lower masses.
- UDGs are *not* special regarding their host halo spin (Fig. 5), in keeping with the thesis of Jiang, Dekel, et al. (2018a) that the spin parameter is not the key factor regulating galaxy size.
- Enforcing NFW-fits, UDG host halos have low concentration parameters (Fig. 5), manifesting that they have cored profiles.
- Most of the UDGs are DM-dominated in the center, with the DM fraction within effective radius $f_{\mathrm{DM,e}} \sim 80\%$ (Fig. 5).
- While the bulk of the NIHAO galaxies are triaxial ($a > b > c$), the UDGs tend to be more prolate ($a \gg b \gtrsim c$) than dwarf galaxies of similar mass and than Milky-Way mass systems (Fig. 7), which are generally oblate or disky ($a \gtrsim b \gg c$). Both simulations and observations imply that galaxies were more prolate when they were more dark matter-dominated (e.g., Ceverino et al. 2016; Zhang et al. 2018). Hence, the prolateness of the UDGs, being DM-dominated, are consistent with such a picture. As shown in the right hand panel of Fig. 6, the Sersic index of UDGs does not correlate with their shape.

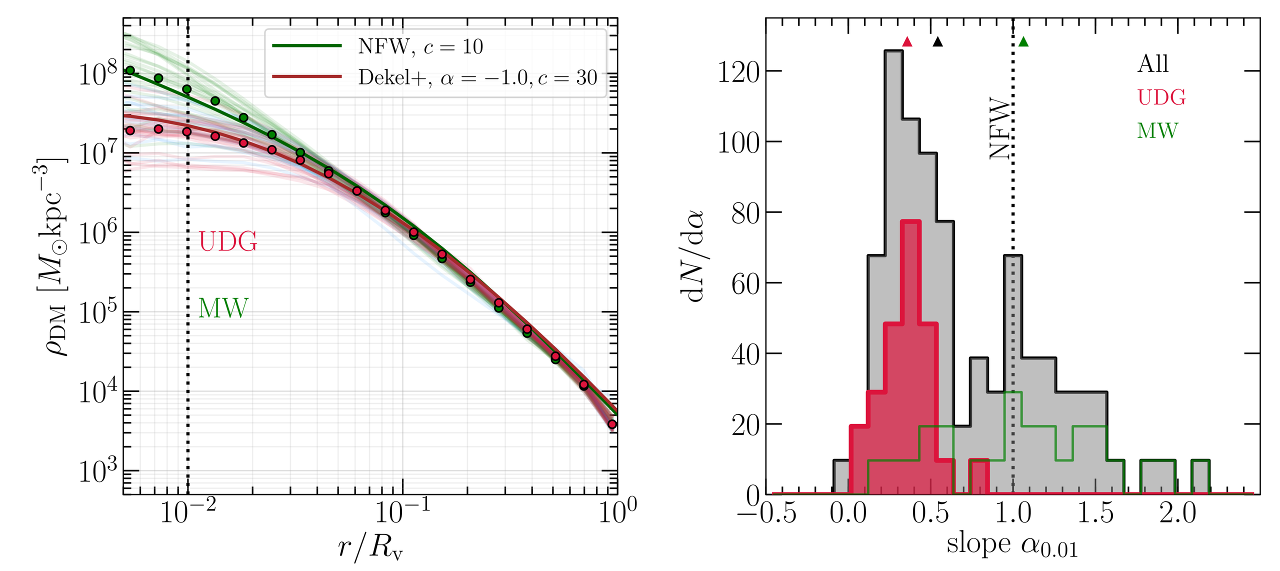

Figure 4. *Left*: Dark matter density profiles of field UDGs in the NIHAO simulations. The thin lines represent the density profiles of individual galaxies (red: UDGs; blue: dwarf galaxies with stellar mass and halo mass similar to UDGs; green: Milky-Way sized galaxies with $M_{vir} > 10^{11.5}M_\odot$). The symbols indicate the medians. Overplotted as reference lines are a NFW profile with a concentration of 10, and a Dekel et al. (2017) profile with $a = -1$ and $c = 30$. *Right*: Distribution of the inner dark matter density slope, $\alpha = -\mathrm{dln}\rho/\mathrm{dln}r$, evaluated at $r = 0.01R_{\mathrm{vir}}$. UDGs (red histogram) show a median slope of ~ 0.35.

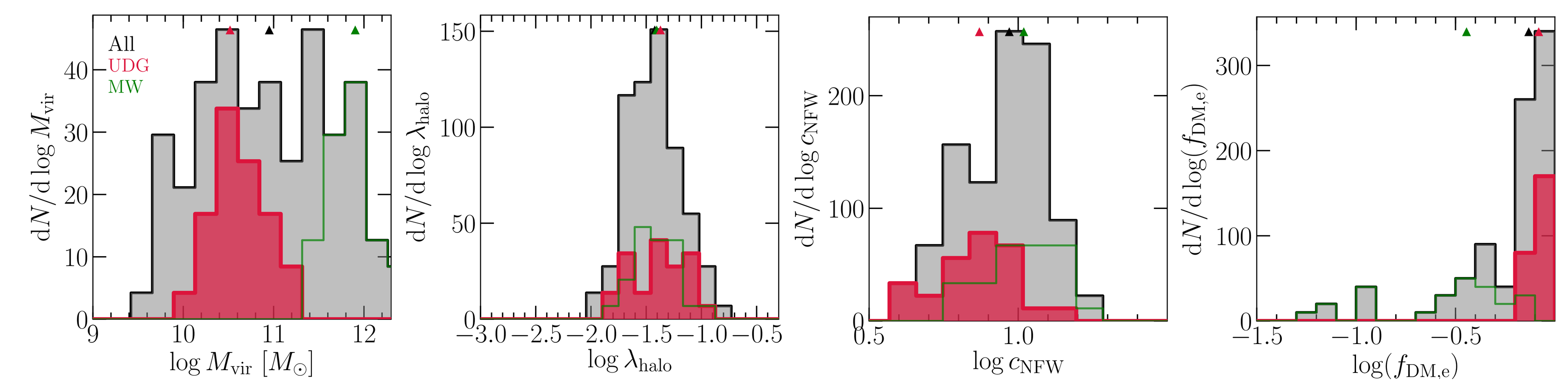

Figure 5. Properties of field-UDG (red) compared to the full NIHAO sample (grey) and to the Milky-Way mass subsample (green), at $z = 0$. The triangles of corresponding color indicate the medians.

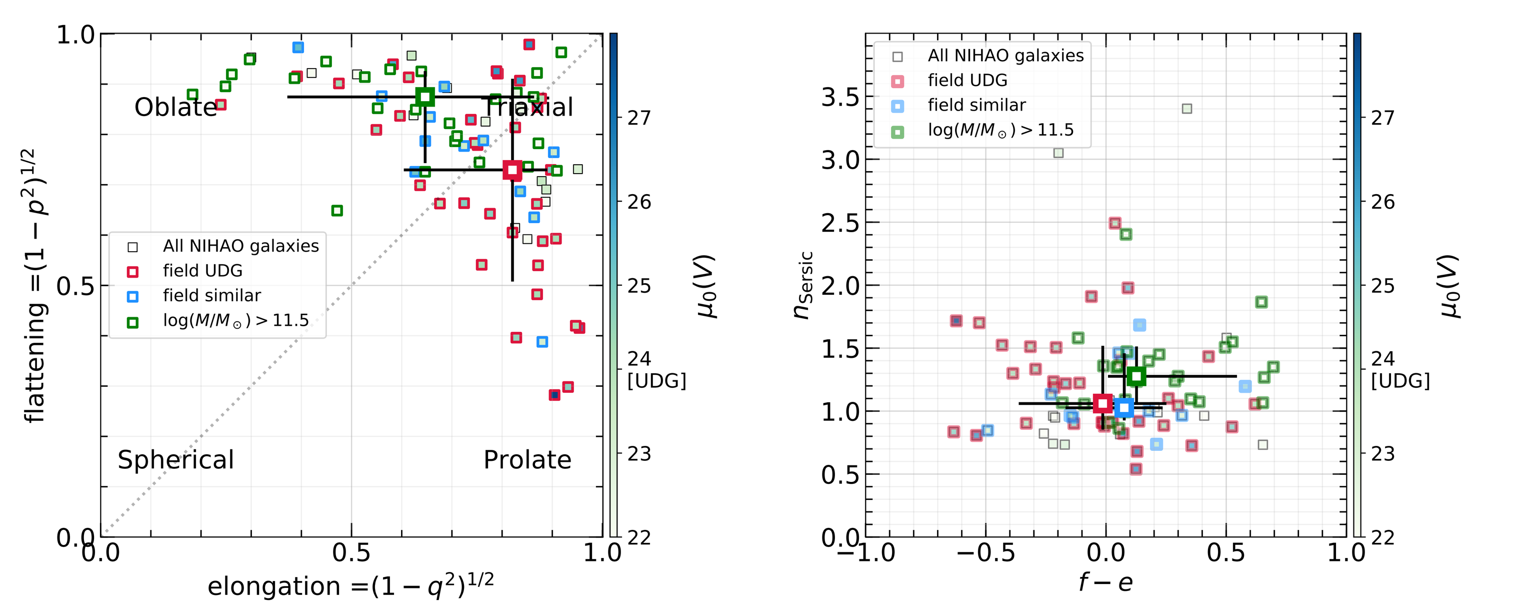

Figure 6. *Left:* Shape of field UDGs compared to the full NIHAO sample and to the Milky Way mass subsample (green). We measure the principal axes ($a > b > c$) of the stars within the effective radius r_{eff}, and define the shape parameters 'flattening' ($f = \sqrt{1 - c^2/b^2}$) and 'elongation' ($e = \sqrt{1 - b^2/a^2}$). Galaxies of different shapes populate different quarters of the space spanned by flattening and elongation. Each small square represents a NIHAO galaxy at $z = 0$, color coded by the central surface brightness in V-band. UDGs, Milky-Ways, and dwarf galaxies of similar mass to UDGs are highlighted with colored edges, in red, green, and blue, respectively. The three big squares with error bars mark the medians and the 16,84th percentiles of the corresponding type. *Right:* Sersic index of field UDGs and other NIHAO galaxies as a function of their shape $f - e$.

The formation of satellite UDGs from tides

We study UDGs in a simulated galaxy group and show that satellite dwarfs can become UDGs after pericenter passage (Jiang, Dekel, Freundlich et al., in prep.):

A galaxy group

- halo 4.2 in Dutton et al. (2015)
- SPH improved Gasoline
- $M_{\mathrm{vir}} \simeq 10^{13.3}M_\odot$
- softening length 600 pc comoving
- Stellar feedback and other physical processes as in the NIHAO simulations

- UDG effective radius r_{eff} and stellar mass $m_\star$ show negligible radial trend (Fig. 7), which is likely the consequence of the combined effect of (1) the disruption of low-mass or diffuse satellite galaxies and (2) of the puffing-up of surviving satellites at orbital pericenters.
- Both the specific star formation rate (sSFR) and B-R color show a trend that UDGs are more quenched towards the center of the galaxy group (Fig. 7), in good agreement with observations (e.g., Alabi et al. 2018). This is indicative of ram pressure stripping, which intensifies towards the center of the dense environment.
- The right hand panel of Fig. 7 shows a representative case study, where the galaxy is puffed up at the first pericenter: (1) r_{eff} increases by a factor of ~ 2; (2) the subhalo mass is stripped to $\sim 1/3$ of the peak value; (3) the stellar mass starts to decrease, indicating that the instantaneous tidal radius at pericenter is smaller than the extent of stars; (4) cold gas is completely stripped at pericenter, suppressing star formation; and Similar behaviors are common among satellite galaxies in the simulated galaxy group, suggesting that a dense environment can transform dwarf galaxies that were not ultra-diffuse at virial-crossing into UDGs, through a combined effect of gas stripping, quenching, and tidal heating.
- Tidal heating can be important for puffing up satellite galaxies (Fig. 8), with the optimal situation being that the stellar content of the satellite reaches the regime between the instantaneous tidal radius at pericenter l_{t} and l_E, an effective truncation radius due to tides operating over a full orbit. Indeed, (1) most of the heating energy is deposited to the outskirts of the satellite at $l > l_E$, which will be stripped after a full orbit; (2) the heating energy injected into the the bound radius l_E is significant, amounting up to $\sim 50\%$ of the binding energy; and (3) tidal heating is minimal in the centermost part of the satellite, at $l < l_{\mathrm{t}}(r_{\mathrm{peri}})$, which is not in the impulsive regime.

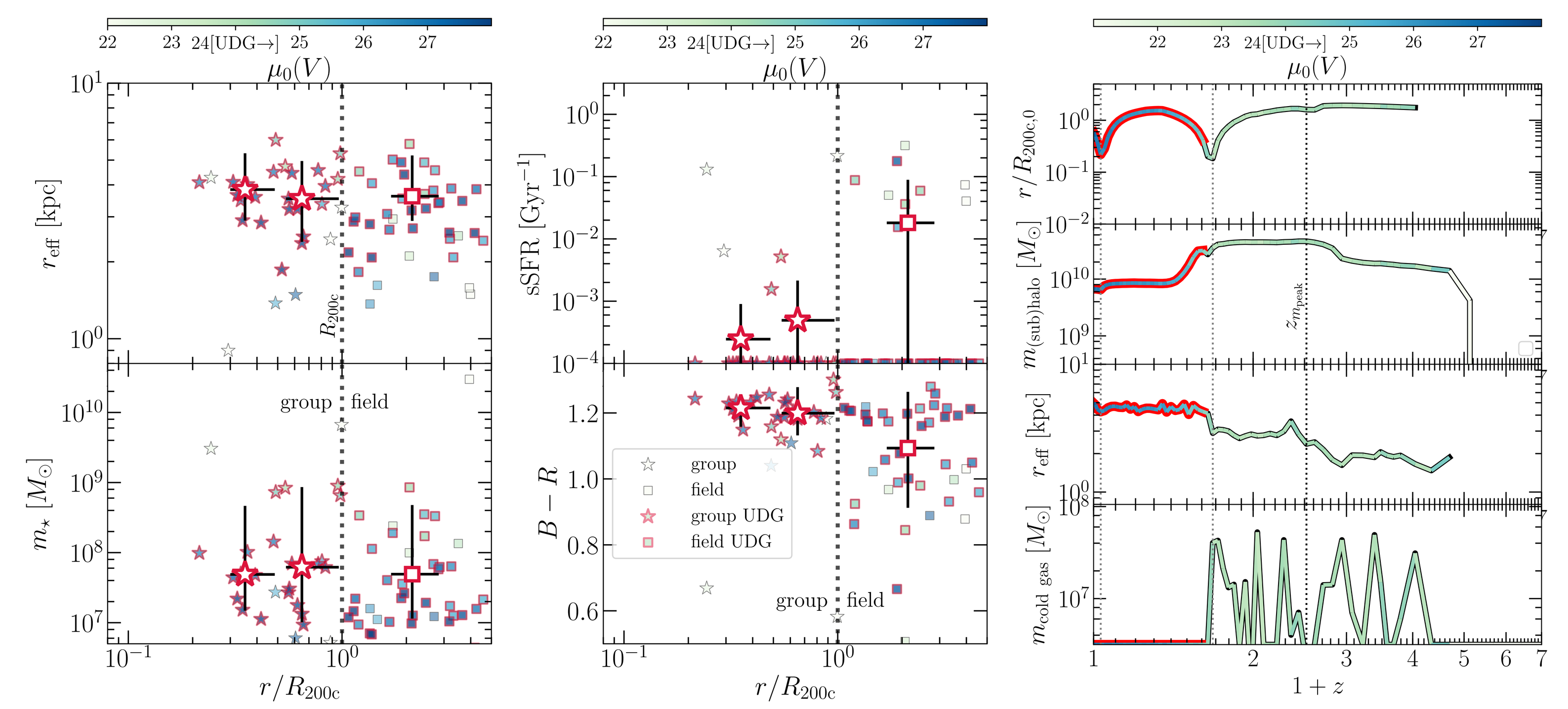

Figure 7. *Left and middle panels:* Properties of UDGs as a function of host-centric distance in a simulated galaxy group ($M_{\mathrm{v}} \simeq 10^{13.3}M_\odot$; Dutton et al. 2015). Galaxies inside and outside the host group's R_{vir} are represented by stars and squares respectively, color coded by the central surface brightness in V band. UDGs are highlighted with red edges. The three big symbols indicate the mean values of UDGs at different distances to the group center – at r/R_{vir} =0-0.5, 0.5-1, and 1.5-3, respectively. The vertical bars indicate the 16 and 84 percentiles; the horizontal bars indicate the radius range. *Right:* An example, showing the evolution a dwarf satellite that becomes a UDG after the first pericenter encounter. Each line represents the history of a quantity, as a function $1 + z$, colored by the central surface brightness and highlighted in red during the UDG-phase. The vertical dotted line indicates the redshift when the halo mass reaches the maximum (approximately first virial-crossing).

Figure 8. Estimate of the tidal heating energy ΔE injected into the bound part of a satellite over a full orbit (from one apocenter to the next) in a galaxy cluster. The specific heating energy at satellite-centric radius l (black) is compared to the local binding energy $E_b(l)$ (red) – their intersection radius (l_E) can be regarded as an effective truncation radius. In comparison, the vertical green line indicates the instantaneous tidal radius $l_{\mathrm{t}}(r_{\mathrm{peri}})$ (King 62) at orbital pericenter. We have assumed an NFW satellite with $m_{\mathrm{vir}} = 10^{11}M_\odot$ and $c = 10$, orbiting an NFW host of $M_{\mathrm{vir}} = 10^{14}M_\odot$ and $c = 5$, with an orbital energy corresponding to a circular orbit of radius R_{vir} and an orbital circularity of 0.5. Tidal heating is computed following Gnedin, Hernquist & Ostriker (1999).

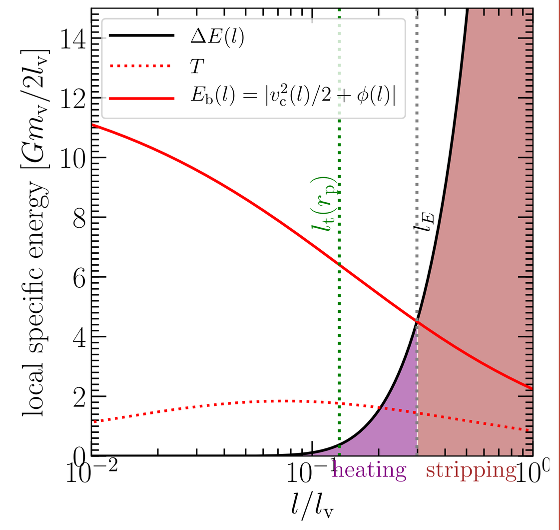

Conclusions

- We present a simple theoretical model to describe the cusp-core transformation of dark matter haloes and the formation of UDGs based on cycles of inflows and outflows, which complements the works of Dutton et al. (2016) and Di Cintio et al. (2017). This model predicts the evolution of the dark matter and stellar density profiles for a single inflow or outflow event, which can be compared to simulations.
- Analyzing field UDGs in the NIHAO simulations, we find that their host haloes have significant cores and typical spins, which favors such UDGs being formed by feedback-induced episodes of inflows and outflows rather than by high-spin haloes. Field UDGs are further dark matter dominated, which reflects on their more prolate shape compared to the overall galaxy distribution.
- Analyzing a simulated galaxy group, we find a dense environment can transform dwarf galaxies into UDGs through a combination of gas stripping, quenching and tidal heating.

References

• Amorisco & Loeb 2015, MNRAS, 459, L51 • Dekel et al. 2017, MNRAS, 468, 1005 • Di Cintio et al. 2017, MNRAS,466, 1 • Dutton et al. 2015, MNRAS,453,2447 • Dutton et al. 2016, MNRAS, 461, 2658 • Gnedin, Hernquist & Ostriker 1999 • Governato et al. 2010, Nature, 463, 203 • Greco et al. 2018, ApJ, 857, 104 • Jiang, Dekel, et al. 2018, arXiv:1804.07306 • Oh et al. 2011, AJ, 141, 193 • Pontzen, A. & Governato, F. 2012, MNRAS, 421, 3464 • Pontzen et al. 2015, MNRAS, 451, 1366 • Teyssier et al. 2013, MNRAS, 429, 3068 • van Dokkum et al. 2015, ApJ, 798, 45 • Wang et al. 2015, MNRAS, 454, 83 •